Inorg. Chem. **2003**, *42*, 1483–1492

Symmetric and Asymmetric Dinuclear Manganese(IV) Complexes Possessing a $[Mn^{IV}_2(\mu\text{-}O)_2(\mu\text{-}O_2CMe)]^{3+}$ Core and Terminal Cl^- Ligands

Sumit Bhaduri,[†] Anastasios J. Tasiopoulos,[†] Milissa A. Bolcar,[‡] Khalil A. Abboud,[†] William E. Streib,[‡] and George Christou*[,†,‡]

Department of Chemistry, University of Florida, Gainesville, Florida 32611-7200, and Department of Chemistry and Molecular Structure Center, Indiana University, Bloomington, Indiana 47405-7102

Received September 19, 2002

The synthesis of new dinuclear manganese(IV) complexes possessing the $[Mn^{IV}_2(\mu\text{-}O)_2(\mu\text{-}O_2CMe)]^{3+}$ core and containing halide ions as terminal ligands is reported. $[Mn_2O_2(O_2CMe)Cl_2(bpy)_2]_2[MnCl_4]$ (**1**; bpy = 2,2′-bipyridine) was prepared by sequential addition of $[MnCl_3(bpy)(H_2O)]$ and $(NBzEt_3)_2[MnCl_4]$ to a CH_2Cl_2 solution of $[Mn_3O_4(O_2CMe)_4(bpy)_2]$. The complex $[Mn^{IV}_2O_2(O_2CMe)Cl(bpy)_2(H_2O)](NO_3)_2$ (**2**) was obtained from a water/acetic acid solution of $MnCl_2\cdot 4H_2O$, bpy, and $(NH_4)_2[Ce(NO_3)_6]$, whereas the $[Mn^{IV}_2O_2(O_2CR)X(bpy)_2(H_2O)](ClO_4)_2$ [X = Cl^- and R = Me (**3**), Et (**5**), or C_2H_4Cl (**6**); and X = F^-, R = Me (**4**)] were prepared by a slightly modified procedure that includes the addition of $HClO_4$. For the preparation of **4**, MnF_2 was employed instead of $MnCl_2\cdot 4H_2O$. $[Mn_2O_2(O_2CMe)Cl_2(bpy)_2]_2[MnCl_4]\cdot 2CH_2Cl_2$ (**1**·$2CH_2Cl_2$) crystallizes in the monoclinic space group *C*2/*c* with $a = 21.756(2)$ Å, $b = 12.0587(7)$ Å, $c = 26.192(2)$ Å, $\alpha = 90°$, $\beta = 111.443(2)°$, $\gamma = 90°$, $V = 6395.8(6)$ Å^3, and $Z = 4$. $[Mn_2O_2(O_2CMe)Cl(H_2O)(bpy)_2](NO_3)_2\cdot H_2O$ (**2**·H_2O) crystallizes in the triclinic space group $P\bar{1}$ with $a = 11.907(2)$ Å, $b = 12.376(2)$ Å, $c = 10.986(2)$ Å, $\alpha = 108.24(1)°$, $\beta = 105.85(2)°$, $\gamma = 106.57(1)°$, $V = 1351.98(2)$ Å^3, and $Z = 2$. $[Mn_2O_2(O_2CMe)Cl(H_2O)(bpy)_2](ClO_4)_2\cdot MeCN$ (**3**·MeCN) crystallizes in the triclinic space group $P\bar{1}$ with $a = 11.7817(7)$ Å, $b = 12.2400(7)$ Å, $c = 13.1672(7)$ Å, $\alpha = 65.537(2)°$, $\beta = 67.407(2)°$, $\gamma = 88.638(2)°$, $V = 1574.9(2)$ Å^3, and $Z = 2$. The cyclic voltammogram (CV) of **1** exhibits two processes, an irreversible oxidation of the $[MnCl_4]^{2-}$ at $E_{1/2} \sim 0.69$ V vs ferrocene and a reversible reduction at $E_{1/2} = 0.30$ V assigned to the $[Mn_2O_2(O_2CMe)Cl_2(bpy)_2]^{+/0}$ couple ($2Mn^{IV}$ to $Mn^{IV}Mn^{III}$). In contrast, the CVs of **2** and **3** show only irreversible reduction features. Solid-state magnetic susceptibility (χ_M) data were collected for complexes **1**·$1.5H_2O$, **2**·H_2O, and **3**·H_2O in the temperature range 2.00–300 K. The resulting data were fit to the theoretical $\chi_M T$ vs T expression for a Mn^{IV}_2 complex derived by use of the isotropic Heisenberg spin Hamiltonian ($\mathcal{H} = -2J\hat{S}_1\hat{S}_2$) and the Van Vleck equation. The obtained fit parameters were (in the format *J*/*g*) –45.0(4) cm^{-1}/2.00(2), –36.6(4) cm^{-1}/1.97(1), and –39.3(4) cm^{-1}/1.92(1), respectively, where J is the exchange interaction parameter between the two Mn^{IV} ions. Thus, all three complexes are antiferromagnetically coupled.

Introduction

The four-electron oxidation of water to form O_2 is a light-driven process that occurs in the complex protein cluster called photosystem II (PSII). This reaction is responsible for nearly all of the atmospheric dioxygen on earth and is catalyzed by the water-oxidizing complex (WOC), which contains an oxide-bridged tetranuclear aggregate, abbreviated hereafter as Mn_4, as well as the cofactors Ca^{2+} and Cl^-.[1−5] Although a crystal structure of the *Synechococcus elongatus* PSII dark-adapted state (designated S_1) at 3.8 Å resolution was reported recently,[6] the precise structure of the WOC is still not clear. Thus, the data from other techniques continues

* Author to whom correspondence should be addressed. E-mail: christou@chem.efl.edu.
[†] University of Florida.
[‡] Indiana University.

(1) *Photosynthetic Water Oxidation*; Nugent, J., Ed.; Special Dedicated Issue; *Biochim. Biophys. Acta: Bioenerg.* **2001**, *1503*, 1−259.
(2) (a) Debus, R. J. *Biochim. Biophys. Acta* **1992**, *1102*, 269 and references therein. (b) *Manganese Redox Enzymes*; Pecoraro, V. L., Ed.; VCH Publishers: New York, 1992. (c) Penner-Hahn, J. E. *Struct. Bonding* **1998**, *90*, 1.
(3) Yachandra, V. K.; Sauer, K.; Klein, M. P. *Chem. Rev.* **1996**, *96*, 2927.
(4) Ruttinger, W.; Dismukes, G. C. *Chem. Rev.* **1997**, *97*, 1.
(5) Tommos, C.; Babcock, G. T. *Acc. Chem. Res.* **1998**, *31*, 18.

10.1021/ic020570v CCC: $25.00
Published on Web 02/06/2003

to be important in providing structural insights into the WOC Mn_4 cluster. EXAFS studies have narrowed down the topological possibilities by identifying the presence in the WOC of $[Mn_2(\mu\text{-}O)_2]$ units, either two[2c,3,7] or perhaps even three.[8] The Mn···Mn separations within these units are 2.7 Å.[2c,3,7] Several structural proposals for the Mn_4 are consistent with extended X-ray absorption fine structure (EXAFS) data: these include (i) some "dimer of dimers" arrangements of two separate $[Mn_2(\mu\text{-}O)_2]$ units linked by a combination of oxide and/or carboxylate bridges (as suggested by the 3.3 Å Mn···Mn separation deduced from EXAFS data)[2c,3,7] and (ii) several Mn_4 topologies comprising two or more vertex- or edge-fused $[Mn_2O_2]$ units.[3,8−10] As a result, it is not surprising that synthetic $[Mn_2(\mu\text{-}O)_2]$-containing species have been, and continue to be the focus of a great deal of study.[11−13]

Also very important to the WOC is the Cl^- ion, which is an essential cofactor of the WOC and is most likely directly bound to the Mn_4.[1−3,14,15] Although many dinuclear complexes possessing the $[Mn_2(\mu\text{-}O)_2]^{z+}$ ($z = 2$, 3, or 4)[11] and $[Mn_2(\mu\text{-}O)_2(\mu\text{-}O_2CR)]^{z+}$ ($z = 2$ or 3)[11j,12,13] cores have been reported, only two of them also contain Cl^- ligands. One is the mixed-valence $Mn^{III}Mn^{IV}$ complex $[Mn_2O_2Cl_2(O_2CMe)(bpy)_2]\cdot 2MeCN$ that was reported by our group,[12a] and the other is the dimanganese(IV) complex $[Mn_2O_2Cl_2(bpea)_2](ClO_4)_2$ [where bpea = *N*,*N*-bis(2-pyridylmethyl)ethylamine].[11j] These two compounds, like most dimanganese complexes containing the $[Mn_2(\mu\text{-}O_2)]$ core, are symmetric. There are just a few examples of di-μ-oxo-dimanganese(III/IV or IV/IV) complexes having an asymmetrical form in which the two Mn ions are coordinated to identical ligands but with different configurations,[11j,k,n,12f] and only two examples, both at the $Mn^{III}Mn^{IV}$ level, of species where the two manganese ions are coordinated to different ligands.[12d]

We herein report the synthesis of a new family of dinuclear Mn^{IV} complexes with the $[Mn_2(\mu\text{-}O)_2(\mu\text{-}O_2CR)]^{3+}$ core (R = Me, Et, or C_2H_4Cl) and terminal halide (Cl^- or F^-) ligands. We also report the crystallographic characterization of three of them, together with the results from electrochemical and magnetochemical studies. These compounds are the first examples of dimanganese complexes possessing the $[Mn^{IV}_2(\mu\text{-}O)_2(\mu\text{-}O_2CR)]^{3+}$ core and terminal Cl^- ligands. In addition, two of the complexes are unusual in being asymmetrical with inequivalent ligands on the two Mn^{IV} ions, a terminal chloride on one Mn and a terminal water molecule on the other, corresponding to the cofactor and substrate, respectively, of the OEC.

Experimental Section

Syntheses. All manipulations were performed under aerobic conditions with materials used as received; water was distilled in-house. $[Mn_3O_4(O_2CMe)_4(bpy)_2]\cdot MeCO_2H$ was available from a previous work.[16] $(NBzEt_3)_2[MnCl_4]$ was prepared in a similar fashion as $[NEt_4]_2[MnCl_4]$.[17] $[MnCl_3(bpy)(H_2O)]$ was prepared by a published procedure.[18] *Caution: perchloric acid and its salts are potentially explosive and should be handled with care*. Elemental analyses were performed by Atlantic Microlab, Inc. (Norcross, GA), and by the in-house facilities of the University of Florida Chemistry Department.

$[Mn_2O_2(O_2CMe)Cl_2(bpy)_2]_2[MnCl_4]$ (1). To a stirred dark brown solution of $[Mn_3O_4(O_2CMe)_4(bpy)_2]\cdot MeCO_2H$ (0.30 g, 0.34 mmol) in 25 mL of CH_2Cl_2 were added $[MnCl_3(bpy)(H_2O)]$ (0.12 g, 0.34 mmol) and $(NBzEt_3)_2[MnCl_4]$ (0.20 g, 0.34 mmol). Stirring was continued for about 20 min; the solution was then filtered and the filtrate was left undisturbed at ambient temperature. After 24 h, the X-ray-quality black crystals (0.09 g) of $\mathbf{1}\cdot 2CH_2Cl_2$ that had formed were collected by filtration, washed with CH_2Cl_2, and dried

(6) Zouni, A.; Witt, H. T.; Kern, J.; Fromme, P.; Krauss, N.; Saenger, W.; Orth, P. *Nature* **2001**, *409*, 739.
(7) Yachandra, V. K.; DeRose, V. J.; Latimer, M. J.; Mukerji, I.; Sauer, K.; Klein, M. P. *Science* **1993**, *260*, 675.
(8) Robblee, J. H.; Messinger, J.; Cinco, R. M.; McFarlane, K. L.; Fernadez, C.; Pizzaro, S. A.; Sauer, K.; Yachandra, V. K. *J. Am. Chem. Soc.* **2002**, *124*, 7459.
(9) Siegbahn, P. E. M. *Inorg. Chem.* **2000**, *39*, 2923.
(10) (a) Peloquin, J. M.; Campbell, K. A.; Randall, D. W.; Evanchik, M. A.; Pecoraro, V. L.; Armstrong, W. H.; Britt, R. D. *J. Am. Chem. Soc.* **2000**, *122*, 10926. (b) Peloquin, J. M.; Britt, R. D. *Biochim. Biophys. Acta* **2001**, *1503*, 96.
(11) (a) Law, N. A.; Kampf, J. W.; Pecoraro, V. L. *Inorg. Chim. Acta* **2000**, *297*, 252. (b) Goodson, P. A.; Oki, A. R.; Glerup, J.; Hodgson, D. J. *J. Am. Chem. Soc.* **1990**, *112*, 6248. (c) Brewer, K. J.; Calvin, M.; Lumpkin, R. S.; Otvos, J. W.; Spreer, L. O. *Inorg. Chem.* **1989**, *28*, 4446. (d) Hagen, K. S.; Armstrong, W. H.; Hope, H. *Inorg. Chem.* **1988**, *27*, 967. (e) Goodson, P. A.; Hodgson, D. J.; Glerup, J.; Michelsen, K.; Weihe, H. *Inorg. Chim. Acta* **1992**, *197*, 141. (f) Goodson, P. A.; Glerup, J.; Hodgson, D. J.; Michelsen, K.; Weihe, H. *Inorg. Chem.* **1991**, *30*, 4909. (g) Larson, E.; Lah, M. S.; Li, X.; Bonadies, J. A.; Pecoraro, V. L. *Inorg. Chem.* **1992**, *31*, 373. (h) Gohdes, J. W.; Armstrong, W. H.; *Inorg. Chem.* **1992**, *31*, 368. (i) Libby, E.; Webb, R. J.; Streib, W. E.; Folting, K.; Huffman, J. C.; Hendrickson, D. N.; Christou, G. *Inorg. Chem.* **1989**, *28*, 4037. (j) Pal, S.; Olmstead, M. M.; Armstrong, W. H. *Inorg. Chem.* **1995**, *34*, 4708. (k) Torayama, H.; Asada, H.; Fujiwara, M.; Matsushita, T. *Polyhedron* **1998**, *17*, 3859. (l) Collomb, M.-N.; Deronzier, A.; Richardot, A.; Pecaut, J. *New J. Chem.* **1999**, *23*, 351. (m) Horner, O.; Charlot, M.-F.; Boussac, A.; Anxolabehere-Mallart, E.; Tchertanov, L.; Guilhem, J.; Girerd, J.-J. *Eur. J. Inorg. Chem.* **1998**, 721. (n) Oki, A. R.; Glerup, J.; Hodgson, D. J. *Inorg. Chem.* **1990**, *29*, 2435. (o) Sarneski, J. E.; Brzezinski, L. J.; Anderson, B.; Didiuk, M.; Manchandra, R.; Crabtree, R. H.; Brudvig, G. W.; Schuttle, G. K. *Inorg. Chem.* **1993**, *32*, 3265. (p) Sarneski, J. E.; Didiuk, M.; Thorp, H. H.; Crabtree, R. H.; Brudvig, G. W.; Faller, J. W.; Schuttle, G. K. *Inorg. Chem.* **1991**, *30*, 2833.
(12) (a) Bashkin, J. S.; Schake, A. R.; Vincent, J. B.; Chang, H.-R.; Li, Q.; Huffman, J. C.; Christou, G.; Hendrickson, D. N. *J. Chem. Soc., Chem. Commun.* **1988**, 700. (b) Wieghardt, K.; Bossek, U.; Zsolnai, G.; Huttner, G.; Blondin, G.; Girerd, J.-J.; Babonneau, F. *J. Chem. Soc., Chem. Commun.* **1987**, 651. (c) Osawa, M.; Fujisawa, K.; Kitajima, N.; Moro-oka, Y. *Chem. Lett.* **1997**, 919. (d) Bossek, U.; Saher, M.; Weyhermuller, T.; Wieghardt, K. *J. Chem. Soc., Chem. Commun.* **1992**, 1780. (e) Schafer, K.-O.; Bittl, R.; Zweygart, W.; Lendzian, F.; Haselhorst, G.; Weyhermuller, T.; Wieghardt, K.; Lubitz, W. *J. Am. Chem. Soc.* **1998**, *120*, 13104. (f) Lal, T. K.; Mukherjee, R. *Inorg. Chem.* **1998**, *37*, 2373. (g) Pal, S.; Gohdes, J. W.; Wilisch, W. C. A.; Armstrong, W. H. *Inorg. Chem.* **1992**, *31*, 713.
(13) (a) Mok, H. J.; Davis, J. A.; Pal, S.; Mandal, S. K.; Armstrong, W. H. *Inorg. Chim. Acta* **1997**, *263*, 385. (b) Dave, B. C.; Czernuszewicz, R. S.; Bond, M. R.; Carrano, C. J. *Inorg. Chem.* **1993**, *32*, 3593. (c) Reddy, K. R.; Rajasekharan, M. V.; Padhye, S.; Dahan, F.; Tuchagues, J.-P. *Inorg. Chem.* **1994**, *33*, 428. (d) Pal, S.; Chan, M. K.; Armstrong, W. H. *J. Am. Chem. Soc.* **1992**, *114*, 6398. (e) Pal, S.; Armstrong, W. H. *Inorg. Chem.* **1992**, *31*, 5417.
(14) Fernandez, C.; Cinco, R. M.; Robblee, J. H.; Messinger, J.; Pizaro, S. A.; Sauer, K.; Yachandra, V. K.; Klein, M. P. In *Photosynthesis: Mechanisms and Effects*; Garab, G., Ed.; Kluwer Academic Publishers: Dordrecht, The Netherlands, 1998; pp 1399−1402.
(15) DeRose, V. J.; Latimer, M. J.; Zimmermann, J.-L.; Mukerji, I.; Yachandra, V. K.; Sauer, K.; Klein, M. P. *Chem. Phys.* **1995**, *194*, 443.
(16) Bhaduri, S.; Pink, M.; Christou, G. *J. Chem. Soc., Chem. Commun.* **2002**, 2352.
(17) Gill, N. S.; Nyholm, R. S. *J. Chem. Soc.* **1959**, 3997.
(18) Goodwin, H. A.; Sylva, R. N. *Aust. J. Chem.* **1965**, *18*, 1743.

Table 1. Crystallographic Data for Complexes **1**·2CH_2Cl_2, **2**·H_2O, and **3**·MeCN

	1	**2**	**3**
empirical formula	$C_{46}H_{42}Cl_{12}Mn_5N_8O_8$[a]	$C_{22}H_{23}ClMn_2N_6O_{12}$[b]	$C_{24}H_{24}Cl_3Mn_2N_5O_{13}$[c]
fw, g/mol	1534.98	708.79	806.71
space group	*C*2/c	$P\bar{1}$	$P\bar{1}$
a, Å	21.756(2)	11.907(2)	11.7817(7)
b, Å	12.0587(7)	12.376(3)	12.2400(7)
c, Å	26.192(2)	10.986(2)	13.1672(7)
β, deg	111.443(2)	105.85(1)	67.407(2)
V, Å^3	6395.8(6)	1351.98(2)	1574.9(2)
Z	4	2	2
T, °C	−80	−170	−80
radiation	Mo Kα	Mo Kα	Mo Kα
ρ_{calcd}, g/cm^3	1.594	1.741	1.701
μ, mm^{-1}	1.514	1.068	1.128
R/*R*1[d,e]	5.79	4.17	4.98
R_w[d,f] or w*R*2[d,g]	14.65[g]	4.52[f]	10.06[g]

[a] Including two CH_2Cl_2 molecules. [b] Including one H_2O molecule. [c] Including one MeCN molecule. [d] $I > 2\sigma(I)$. [e] $R = R1 = 100\sum(||F_o| - |F_c||)/\sum|F_o|$. [f] $R_w = 100[\sum w(|F_o| - |F_c|)^2/\sum w|F_o|^2]^{1/2}$, where $w = 1/\sigma^2(|F_0|)$. [g] $wR2 = 100[\sum[w(F_o^2 - F_c^2)^2]/\sum[w(F_o^2)^2]]^{1/2}$, where $w = 1/[\sigma^2(F_o^2) + [(ap)^2 + bp]$, where $p = [\max(F_o^2, 0) + 2F_c^2]/3$.

in vacuo. The yield was 25% based on total bpy. Anal. Calcd (Found) for **1**·1.5H_2O: C, 37.96 (37.72); H, 2.97 (2.73); N, 8.05 (7.88). Selected IR bands (KBr, cm^{-1}): 3425 (m, br), 3105 (w), 3070 (w), 1601 (s), 1570 (w),1496 (s), 1468 (m), 1447 (s), 1311 (m), 1267 (w), 1247 (w), 1158 (w), 1105 (w), 1071 (w), 1057(w), 1036 (m), 1025 (w), 770 (s), 726 (m), 694 (m), 672 (s), 656 (m), 638 (m), 595 (m), 420 (m).

[$Mn_2O_2(O_2CMe)Cl(H_2O)(bpy)_2$]($NO_3$)$_2$ (2). To a stirred yellow solution of $MnCl_2$·4H_2O (1.98 g, 10.0 mmol) and bpy (1.56 g, 10.0 mmol) in H_2O/$MeCO_2H$ (100 mL/30 mL) was slowly added an orange solution of $(NH_4)_2[Ce(NO_3)_6]$ (11.02 g, 20.10 mmol) in H_2O/$MeCO_2H$ (33 mL/10 mL), resulting in a dark brown solution. The solution was rotary-evaporated at 40 °C to half of its original volume and left undisturbed for 24 h at ambient temperature. The resulting X-ray-quality black crystals were collected by filtration, washed with H_2O, EtOH, and Et_2O, and dried in air. The yield was 2.63 g (74%). Anal. Calcd (Found) for **2**·H_2O: C, 37.30 (36.95); H, 3.27 (3.15); N, 11.90 (11.67); Cl, 5.00 (5.25); Mn, 15.50 (15.75). Selected IR data (KBr, cm^{-1}): 3446 (s, br), 3100 (w), 3079 (w) 1602 (m), 1575 (w), 1559 (w), 1498 (m), 1470 (m), 1446 (s), 1420 (m), 1384 (s), 1312 (m), 1249 (w), 1156 (w), 1104 (w), 1073 (w), 1060 (w), 1036 (m), 1024 (w), 770 (s), 725 (m), 696 (m), 672 (m), 655 (m), 637 (m), 614 (m), 539 (w), 419 (w).

[$Mn_2O_2(O_2Me)Cl(H_2O)(bpy)_2$]($ClO_4$)$_2$ (3). To a pale brown solution of $MnCl_2$·4H_2O (0.59 g, 2.98 mmol) and bpy (0.47 g, 3.0 mmol) in H_2O/$MeCO_2H$ (30 mL/4.5 mL) was added an orange solution of $(NH_4)_2[Ce(NO_3)_6]$ (3.30 g, 6.02 mmol) in H_2O/$HClO_4$ (70%) (15 mL/3 mL), resulting in a brown solution. After 24 h at ambient temperature, a green-brown powder was collected by filtration, washed with EtOH and Et_2O, and dried in air. The yield was 0.99 g (85%). Recrystallization from MeCN/Et_2O gave black crystals of **3**·MeCN. Anal. Calcd (Found) for **3**·H_2O: C, 33.71 (33.90); H, 2.96 (2.80); N, 7.15 (7.30). Selected IR data (KBr, cm^{-1}): 3431 (s, br), 3079 (w), 1602 (s), 1571 (w), 1559 (w), 1500 (m), 1467 (m), 1446 (s), 1405 (m), 1384 (w), 1353 (w), 1312 (m), 1271 (w), 1249 (w), 1180 (w), 1120 (s), 1103 (s), 1085 (s), 1035 (m), 770 (s), 724 (m), 695 (m), 677 (m), 654 (m), 624 (s), 535 (w), 435 (w), 419 (m).

[$Mn_2O_2(O_2CMe)F(H_2O)(bpy)_2$]($ClO_4$)$_2$ (4). The procedure that was employed for **3**·H_2O was repeated with MnF_2 in place of $MnCl_2$·4H_2O. The yield of complex **4** was 0.80 g (70%). Anal. Calcd (Found) for **4**·H_2O: C, 34.44 (34.20); H, 3.02 (2.95); N, 7.30 (7.40). Selected IR data (KBr, cm^{-1}): 3396 (s, br), 3105 (w), 3080 (w), 1601 (s), 1571 (w), 1497 (s), 1469 (m), 1446 (s), 1310 (m), 1273 (w), 1245 (w), 1120 (s), 1103 (s), 1086 (s), 1035 (m), 854 (m), 770 (m), 727 (m), 695 (s), 669 (m), 654 (m), 625 (s), 470 (m), 419 (m).

[$Mn_2O_2(O_2CEt)Cl(H_2O)(bpy)_2$]($ClO_4$)$_2$ (5). The procedure that was employed for **3**·H_2O was repeated with propionic acid instead of acetic acid. The yield was 84%. Anal. Calcd (Found) for **5**·H_2O: C, 34.63 (34.37); H, 3.16 (3.35); N, 7.02 (7.03). Selected IR data (KBr, cm^{-1}): 3440 (s, br), 3082 (w), 1601 (s), 1575 (w), 1540 (w), 1499 (m), 1466 (m), 1447 (s), 1422 (m), 1381 (w), 1310 (m), 1271 (w), 1249 (w), 1120 (s), 1106 (s), 1090 (s), 1036 (m), 923 (w), 772 (s), 725 (m), 677 (m), 667(m), 655 (m), 627 (s), 532 (w), 440 (w), 418 (w).

[$Mn_2O_2(O_2CC_2H_4Cl)Cl(H_2O)(bpy)_2$]($ClO_4$)$_2$ (6). To a pale yellow-brown solution of $MnCl_2$·4H_2O (0.40 g, 2.0 mmol), bpy (0.32 g, 2.0 mmol), and 3-chloropropionic acid (2.51 g, 23.3 mmol) in H_2O (30 mL) was added an orange solution of $(NH_4)_2[Ce(NO_3)_6]$ (2.21 g, 4.03 mmol) in H_2O/$HClO_4$ (70%) (10 mL/2 mL), resulting in a dark brown solution. Within minutes, a precipitate began to form. After 24 h at ambient temperature, the green-brown powder was collected by filtration, washed with H_2O, EtOH, and Et_2O, and dried in air. The yield was 0.58 g (70%). Anal. Calcd (Found) for **6**·H_2O: C, 33.20 (33.33); H, 2.91 (3.17); N 6.73 (6.88). Selected IR data (KBr, cm^{-1}): 3430 (s, br), 3084 (w), 1601(m), 1570 (w), 1540 (w), 1498 (m), 1470 (m), 1447 (s), 1384 (w), 1312 (m), 1248 (w), 1143 (s), 1109 (s), 1089 (s), 1036(m), 1024 (m), 930 (w), 849 (w), 770 (s), 727 (m), 677 (m), 667 (m), 656 (m), 636 (m), 627 (s), 493 (w), 451 (w), 419 (w).

X-ray Crystallography. Data for complexes **1**·2CH_2Cl_2 and **3**·MeCN were collected at the University of Florida at 193 K on a Siemens Smart Platform equipped with a CCD area detector and a graphite monochromator utilizing Mo Kα radiation ($\lambda = 0.71073$ Å). Data collection parameters are listed in Table 1. Cell parameters were refined by use of up to 8192 reflections. A full sphere of data (1381 frames) was collected by the ω-scan method (0.3° frame width). The first 50 frames were remeasured at the end of data collection to monitor instrument and crystal stability (maximum correction on *I* was < 1%). An absorption correction by integration was applied, based on measured indexed crystal faces.

The structures were solved by direct methods in SHELXTL5 and refined by full-matrix least squares. Non-hydrogen atoms were refined anisotropically, whereas the hydrogen atoms were placed in ideal, calculated positions, with isotropic thermal parameters riding on their respective carbon atoms. For complex **1**·2CH_2Cl_2, the asymmetric unit consists of a Mn_2 cation, half a $[MnCl_4]^{2-}$

anion, and a CH_2Cl_2 molecule disordered over three positions. After refininement of the site occupation factors of the three positions, they were fixed at 0.4, 0.4, and 0.2. A total of 388 parameters were refined in the final cycles of refinement on F^2. For **3**·MeCN, the asymmetric unit contains one Mn_2 cation, two perchlorate anions, and one molecule of MeCN. The water H atoms were obtained from a difference Fourier map and refined without any constraints. The H atoms on C9 were clearly disordered; two sets of methyl H atoms were treated as riding on C9, and their site occupation factors were fixed at 0.5. A total of 434 parameters were refined in the final cycles of refinement on F^2.

Data for **2**·H_2O were collected on a Picker four-circle diffractometer at 103 K at the facilities of the Indiana University Molecular Structure Center. Data collection parameters are listed in Table 1. Details of the diffractometry, low-temperature facilities, and computational procedures employed by the Indiana University Molecular Structure Center are available elsewhere.[19] The structure was solved by a combination of direct methods (MULTAN78) and Fourier techniques. The positions of the atoms in an $Mn_2O_5N_2C_{12}$ portion of the structure were obtained from an initial E-map. The positions of the remaining atoms, including all of the hydrogens, were obtained from subsequent iterations of least-squares refinement and difference Fourier map calculation. The asymmetric unit contains the complete Mn_2 cation, two nitrate anions, and one molecule of water.

Final values of the discrepancy indices $R(R_w)$ or $R1(wR2)$ for the three structures are included in Table 1.

Physical Measurements. IR spectra were recorded on KBr pellets in a Nicolet Nexus 670 spectrophotometer. Cyclic voltammetry was performed on ~1.0 mM solutions at a 100 mV/s scan rate with a BAS CV-50W voltammetric analyzer and a standard three-electrode assembly (glassy-carbon working electrode, Pt wire auxiliary electrode, $Ag/AgNO_3$ reference electrode), with 0.1 M $NBu^n_4PF_6$ as supporting electrolyte. Potentials are quoted versus the ferrocene/ferrocenium couple under the same conditions. DC magnetic susceptibility data were collected on powdered, microcrystalline samples on a Quantum Design MPMS-XL SQUID magnetometer equipped with a 7 T (70 kG) magnet and capable of operating in the 1.8−400 K range. A diamagnetic correction to the observed susceptibilities was applied using Pascal's constants.

Results and Discussion

Syntheses. Two methods were employed for the preparation of the complexes obtained in this work. The first is the reaction of $[Mn_3O_4(O_2CMe)_4(bpy)_2]$ with mononuclear $[MnCl_3(bpy)(H_2O)]$ and either $(NBu^n_4)ClO_4$ or $(NBzEt_3)_2[MnCl_4]$ in CH_2Cl_2, while the second is the oxidation of Mn^{II} reagents with Ce^{IV} in the presence of bpy in an aqueous carboxylic acid medium. Both methods were found to give dinuclear Mn^{IV} products.

$[Mn_3O_4(O_2CMe)_4(bpy)_2]$ is a $3Mn^{IV}$ complex and contains a V-shaped $[Mn(\mu\text{-}O)_2Mn(\mu\text{-}O)_2Mn]^{4+}$ core. It was only recently prepared[16] and has since been under detailed investigation by various spectroscopic and physical techniques for its potential relevance as a fragment of the Mn_4 cluster of the OEC. We have also been studying its use as a reagent in a variety of reactions. In one such reaction with an equimolar amount of $[MnCl_3(bpy)(H_2O)]$ and $(NBu^n_4)ClO_4$, the product was a mixture of $[Mn_2O_2(O_2CMe)Cl_2(bpy)_2]_2[MnCl_4]$ (**1**), obtained in low yield as well-formed black crystals of **1**·$2CH_2Cl_2$, and its perchlorate analogue. Once the identity of **1** and the presence of $[MnCl_4]^{2-}$ anions had been established by crystallography, the compound was obtained in pure form, and with an improved yield of 25%, by addition to the reaction mixture of $(NBzEt_3)_2[MnCl_4]$ instead of $(NBu^n_4)ClO_4$. However, the reaction is still clearly a complicated one, and there are likely several species present in equilibrium in solution; the low solubility of **1** allows its isolation in pure form from this mixture. Charge considerations and the metric parameters from the crystal structure (see below) establish that the cation of **1** contains two Mn^{IV} ions and the anion contains Mn^{II}. Since the starting material $[Mn_3O_4(O_2CMe)_4(bpy)_2]$ already contains Mn^{IV}, and the required $[MnCl_4]^{2-}$ was added to the reaction, the primary contribution of the $[MnCl_3(bpy)(H_2O)]$ to the formation of **1** appears to be to act as a source of Cl^- and bpy, as summarized in

$$4[Mn_3O_4(O_2CMe)_4(bpy)_2] + 4[MnCl_3(bpy)(H_2O)] + 3[MnCl_4]^{2-} \rightarrow 3[Mn_2O_2(O_2CMe)Cl_2(bpy)_2]_2[MnCl_4] + 10MeCO_2^- + 8OH^- + 4Mn^{3+} \quad (1)$$

Ce^{IV} is a strong one-electron oxidant ($E° = 1.61$ V vs NHE) and it is quite capable of oxidizing Mn^{II} to Mn^{III} or Mn^{IV}. In fact, Ce^{IV} has been used previously to prepare some higher oxidation state Mn complexes,[13c,20] as well as being the oxidant in water oxidation studies in which Ru complexes were the catalysts.[4,21] We have also used Ce^{IV} to prepare the mixed-valent ($3Co^{III}$, Co^{IV}) complexes $[Co_4O_4(O_2CR)_2(bpy)_4]^{3+}$ by the one-electron oxidation of $[Co_4O_4(O_2CR)_2(bpy)_4]^{2+}$.[22] In the present work, a solvent system comprising aqueous carboxylic acid was employed for the reactions of $(NH_4)_2[Ce(NO_3)_6]$ with Mn^{II} salts. The carboxylic acid helps maintain an acidic environment so that formation of manganese oxides and/or hydroxides is prevented. In addition, the solvent provides a plentiful supply of carboxylate ions as potential ligands in the products.

The addition of 2 equiv of $(NH_4)_2[Ce(NO_3)_6]$ to a $H_2O/MeCO_2H$ solution of $MnCl_2·4H_2O$ and bpy resulted in the formation of $[Mn_2O_2(O_2CMe)Cl(H_2O)(bpy)_2](NO_3)_2$ (**2**) as essentially black crystals of **2**·H_2O:

$$2MnCl_2 + 2bpy + MeCO_2H + 3H_2O - 4e^- \rightarrow [Mn_2O_2(O_2CMe)Cl(H_2O)(bpy)_2]^{2+} + 3Cl^- + 5H^+ \quad (2)$$

The corresponding ClO_4^- salt (**3**) of the same dinuclear cation was obtained by a slightly modified procedure that involved the addition of perchloric acid to the reaction solution. This

(19) Chisholm, M. H.; Folting, K.; Huffman, J. C.; Kirkpatrick, C. C. *Inorg. Chem.* **1984**, *23*, 1021.

(20) (a) Reddy, K. R.; Rajasekharan, M. V.; Arulsamy, N.; Hodgson, D. J. *Inorg. Chem.* **1996**, *35*, 2283. (b) Reddy, K. R.; Rajasekharan, M. V. *Polyhedron* **1994**, *13*, 765.

(21) (a) Yagi, M.; Kaneko, M. *Chem. Rev.* **2001**, *101*, 21. (b) Gilbert, J. A.; Eggleston, D. S.; Murphy, W. R.; Geselowitz, D. A.; Gersten, S. W.; Hodgson, D. J.; Meyer, T. J. *J. Am. Chem. Soc.* **1985**, *107*, 3855.

(22) (a) Dimitrou, K.; Brown, A. D.; Folting, K.; Christou, G. *Inorg. Chem.* **1999**, *38*, 1834. (b) Dimitrou, K.; Brown, A. D.; Concolino, T. E.; Rheingold, A. L.; Christou, G. *Chem. Commun.* **2001**, 1284.

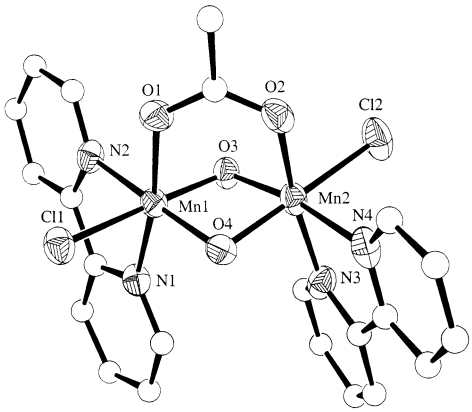

Figure 1. ORTEP representation of the cation of **1** at the 50% probability level.

Table 2. Selected Interatomic Distances and Angles for **1**·2CH_2Cl_2[a]

Mn(1)−O(4)	1.790(3)	Mn(2)−O(3)	1.795(3)
Mn(1)−O(3)	1.820(4)	Mn(2)−O(4)	1.822(4)
Mn(1)−O(1)	1.942(4)	Mn(2)−O(2)	1.948(4)
Mn(1)−N(1)	1.996(4)	Mn(2)−N(3)	1.994(5)
Mn(1)−N(2)	2.044(4)	Mn(2)−N(4)	2.038(5)
Mn(1)−Cl(1)	2.2821(16)	Mn(2)−Cl(2)	2.2638(17)
Mn(3)−Cl(6#1)	2.3590(19)	Mn(3)−Cl(6)	2.3590(19)
Mn(3)−Cl(5#1)	2.364(2)	Mn(3)−Cl(5)	2.364(2)
Mn(1)···Mn(2)	2.6715(11)		
O(4)−Mn(1)−O(3)	83.09(16)	O(3)−Mn(2)−O(4)	82.91(16)
O(4)−Mn(1)−O(1)	93.43(16)	O(3)−Mn(2)−O(2)	93.60(16)
O(3)−Mn(1)−O(1)	90.73(16)	O(4)−Mn(2)−O(2)	90.59(16)
O(4)−Mn(1)−N(1)	95.60(18)	O(3)−Mn(2)−N(3)	96.31(18)
O(3)−Mn(1)−N(1)	93.42(17)	O(4)−Mn(2)−N(3)	90.73(18)
O(1)−Mn(1)−N(1)	170.46(18)	O(2)−Mn(2)−N(3)	170.09(18)
O(4)−Mn(1)−N(2)	171.27(17)	O(3)−Mn(2)−N(4)	169.56(18)
O(3)−Mn(1)−N(2)	89.89(17)	O(4)−Mn(2)−N(4)	87.61(17)
O(1)−Mn(1)−N(2)	91.85(17)	O(2)−Mn(2)−N(4)	90.84(19)
N(1)−Mn(1)−N(2)	79.57(19)	N(3)−Mn(2)−N(4)	79.4(2)
O(4)−Mn(1)−Cl(1)	93.75(12)	O(3)−Mn(2)−Cl(2)	95.22(12)
O(3)−Mn(1)−Cl(1)	176.76(12)	O(4)−Mn(2)−Cl(2)	178.04(12)
O(1)−Mn(1)−Cl(1)	88.74(12)	O(2)−Mn(2)−Cl(2)	90.10(13)
N(1)−Mn(1)−Cl(1)	87.60(13)	N(3)−Mn(2)−Cl(2)	88.91(14)
N(2)−Mn(1)−Cl(1)	93.32(13)	N(4)−Mn(2)−Cl(2)	94.22(14)
Mn(1)−O(4)−Mn(2)	95.38(16)	Mn(2)−O(3)−Mn(1)	95.30(17)
Cl(6#1)−Mn(3)−Cl(5#1)	112.45(8)	Cl(6#1)−Mn(3)−Cl(6)	110.01(11)
Cl(6#1)−Mn(3)−Cl(5)	106.32(8)	Cl(6)−Mn(3)−Cl(5#1)	106.32(8)
Cl(5#1)−Mn(3)−Cl(5)	109.39(16)	Cl(6)−Mn(3)−Cl(5)	112.45(8)

[a] Distances are given in angstroms; angles are given in degrees.

latter procedure was also successfully employed for the preparation of the propionate and the 3-chloropropionate complexes **5** and **6**, respectively.

It was also found that the syntheses could be extended to F^--containing species. When MnF_2 was employed as the Mn^{II} source in place of $MnCl_2·4H_2O$, a dark brown crystalline precipitate of **4**·H_2O was isolated. Unfortunately, we have not as yet been able to obtain **4** in a form suitable for crystallography.

Description of Structures. Crystallographic data collection and structure refinement details for **1**·2CH_2Cl_2, **2**·H_2O, and **3**·MeCN are summarized in Table 1.

For $[Mn_2O_2(O_2CMe)Cl_2(bpy)_2]_2(MnCl_4)$ (**1**·2CH_2Cl_2), an ORTEP representation of the cation is shown in Figure 1 and selected interatomic distances and angles are collected in Table 2. The asymmetric unit of **1** consists of a complete Mn_2 cation and half a $[MnCl_4]^{2-}$ anion, as well as disordered CH_2Cl_2. Thus, the cation-to-anion ratio is 2:1. The two Mn^{IV} ions of the dinuclear cation are bridged by two μ-O^{2-} ions and one μ-$MeCO_2^-$ group. Octahedral coordination at each Mn ion is completed by a chelating bpy group and a terminal Cl^- ion. The two Cl^- ligands are approximately trans about the Mn···Mn vector [torsion angle Cl(1)−Mn(1)−Mn(2)−Cl(2) = 161.0(1)°]. The longer Mn(1)−O(3) [1.820(4) Å] and Mn(2)−O(4) [1.822(4) Å] distances compared with Mn(1)−O(4) [1.790(3) Å] and Mn(2)−O(3) [1.795(3) Å] are indicative of a greater trans influence of Cl^- over bpy nitrogen. There are only three other examples of complexes that contain the $[Mn_2(\mu\text{-}O)_2Cl_2]$ unit with terminal chloride ligands attached to the Mn ions: (i) the $Mn^{IV}{}_2$ complex $[Mn_2O_2Cl_2(bpea)_2]^{2+}$,[11j] (ii) the mixed-valence $Mn^{III}Mn^{IV}$ complex $[Mn_2O_2Cl_2(O_2CMe)(bpy)_2]$,[12a] and (iii) $[Mn_3O_4Cl_2(bpy)_4]^{2+}$.[23] The elongation of the Mn−O bonds trans to the coordinated chloride ligands is unequivocal in the latter two cases, but not in the first. The Mn^{IV}−Cl bond lengths in **1** [2.2821(16) and 2.2638(17) Å] are similar to those in example i [2.273(2) Å] but shorter than those for examples ii [2.3414(26) Å] and iii [2.336(5) Å]. The Mn···Mn separation [2.6715(11) Å] is slightly longer than the upper limit of the range (2.580−2.642 Å) observed for other structurally characterized complexes with the $[Mn^{IV}{}_2O_2(O_2CMe)]^{3+}$ core.[12e,13] Owing to the bridging acetate group, the $[Mn_2O_2]$ core of **1** is not planar [dihedral angle between the O(4)−Mn(1)−O(3) and O(4)−Mn(2)−O(3) planes is 161.6(1)°], as is also the case for other complexes with this triply bridged core.[11j,12,13]

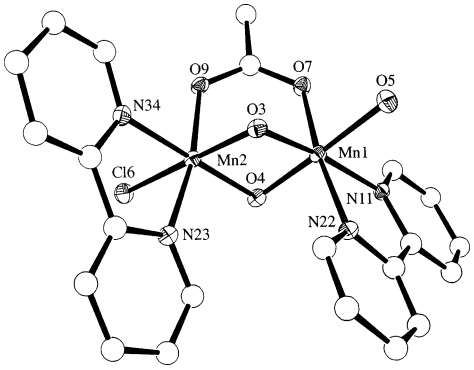

Figure 2. ORTEP representation of the cation of **2** at the 50% probability level.

For $[Mn_2O_2(O_2CMe)Cl(H_2O)(bpy)_2](NO_3)_2·H_2O$ (**2**·H_2O), a labeled ORTEP plot of the cation is shown in Figure 2, and selected interatomic distances and angles are listed in Table 3.

The cation consists of two Mn^{IV} ions triply bridged by two μ-oxide ions, O(3) and O(4), and one μ-acetate group. Distorted octahedral geometry at each Mn is completed by a bpy group and either a water molecule [at Mn(1)] or a Cl^- ion [at Mn(2)]. The Mn(1)−water bond length [Mn(1)−O(5) = 1.959(3) Å] is slightly shorter than the average Mn^{IV}−OH_2 bond lengths of 1.984(2), 1.991(5), and 2.011(2) Å reported for $[Mn_2O_2(O_2CMe)(bpy)_2(H_2O)_2]^{3+}$ ($2Mn^{IV}$)[13b,c] and the mixed-valence (Mn^{III}/Mn^{IV}) complex $[Mn_2O_2(terpy)_2$-

(23) Auger, N.; Girerd, J.-J.; Corbella, M.; Gleizes, A.; Zimmerman, J.-L. *J. Am. Chem. Soc.* **1990**, *112*, 448.

Table 3. Selected Interatomic Distances and Angles for **2**·H_2O[a]

Mn(1)−O(3)	1.7955(28)	Mn(2)−O(3)	1.848(3)
Mn(1)−O(4)	1.800(3)	Mn(2)−O(4)	1.809(3)
Mn(1)−O(5)	1.959(3)	Mn(2)−Cl(6)	2.2643(13)
Mn(1)−O(7)	1.947(3)	Mn(2)−O(9)	1.937(3)
Mn(1)−N(11)	2.046(4)	Mn(2)−N(34)	2.048(4)
Mn(1)−N(22)	2.005(3)	Mn(2)−N(23)	1.998(3)
Mn(1)···Mn(2)	2.6702(13)		

O(3)−Mn(1)−O(4)	84.46(13)	Cl(6)−Mn(2)−O(3)	176.44(9)
O(3)−Mn(1)−O(5)	93.74(14)	Cl(6)−Mn(2)−O(4)	94.31(10)
O(3)−Mn(1)−O(7)	93.51(12)	Cl(6)−Mn(2)−O(9)	88.54(9)
O(3)−Mn(1)−N(11)	173.09(13)	Cl(6)−Mn(2)−N(23)	86.48(10)
O(3)−Mn(1)−N(22)	93.99(13)	Cl(6)−Mn(2)−N(34)	92.93(10)
O(4)−Mn(1)−O(5)	177.93(14)	O(3)−Mn(2)−O(4)	82.69(13)
O(4)−Mn(1)−O(7)	91.00(12)	O(3)−Mn(2)−O(9)	89.76(12)
O(4)−Mn(1)−N(11)	92.48(13)	O(3)−Mn(2)−N(23)	95.66(13)
O(4)−Mn(1)−N(22)	92.58(13)	O(3)−Mn(2)−N(34)	90.24(13)
O(5)−Mn(1)−O(7)	88.11(13)	O(4)−Mn(2)−O(9)	94.21(12)
O(5)−Mn(1)−N(11)	89.42(14)	O(4)−Mn(2)−N(23)	94.86(14)
O(5)−Mn(1)−N(22)	88.54(14)	O(4)−Mn(2)−N(34)	170.88(13)
O(7)−Mn(1)−N(11)	92.73(13)	O(9)−Mn(2)−N(23)	169.96(13)
O(7)−Mn(1)− N(22)	171.96(13)	O(9)−Mn(2)−N(34)	91.51(13)
N(11)−Mn(1)−N(22)	79.94(14)	N(23)−Mn(2)−N(34)	80.06(14)
Mn(1)−O(3)−Mn(2)	94.24(13)	Mn(1)−O(4)−Mn(2)	95.43(14)

[a] Distances are given in angstroms; angles are given in degrees.

$(H_2O)_2]^{2+}$ [11] (terpy = 2,2′:6′,2″-terpyridine), but it is still much longer than terminal Mn^{IV}−OH bond lengths of 1.830(4)[13d,e] and 1.881(5) Å,[24] confirming that the bound species in **2** is an aqua group. The Mn(2)−Cl bond length of 2.2643(13) Å is similar to those in **1**. Again, the longer Mn(2)−O^{2-} bond is that trans to the chloride ion [Mn(2)−O(3) = 1.848(3) Å, Mn(2)−O(4) = 1.809(3) Å], whereas the Mn(1)−O^{2-} bond lengths are equal [Mn(1)−O(3) = 1.796(3) Å, Mn(1)−O(4) = 1.800(3) Å]. The Mn(1)···Mn(2) distance [2.6702(13) Å] is also similar to that in **1** [2.6715(11) Å]. The $[Mn_2O_2]$ unit of **2** is again not planar, the dihedral angle between the planes O(3)−Mn(1)−O(4) and O(3)−Mn(2)−O(4) being 161.8(1)°, the same as that in **1**.

A careful examination of the unit cell of **2**·H_2O reveals the presence of hydrogen-bonding interactions. The bound H_2O molecule is hydrogen-bonded to O(37) of a NO_3^- anion [O(5)···O(37) = 2.570(5) Å] and O(43) of the lattice H_2O molecule [O(5)···O(43) = 2.602(5) Å] (Figure 3). The latter is also hydrogen-bonded to O(40) of the second NO_3^- anion [O(43)···O(40) = 2.781(5) Å] and one of the bridging oxide ions, O(3), of a neighboring molecule of **2** [O(43)···O(3) = 2.869(5) Å]. The O···O distances and O−H···O angles [163(6)−175(6)°] are indicative of strong hydrogen bonds.

For $[Mn_2O_2(O_2CMe)Cl(H_2O)(bpy)_2](ClO_4)_2$·MeCN (**3**·MeCN), an ORTEP representation is shown in Figure 4 and selected interatomic distances and angles are listed in Table 4.

The complex is structurally very similar to **2**·H_2O except that (i) the anion in **3** is perchlorate rather than nitrate, as in **2,** and (ii) the asymmetric unit contains an MeCN molecule instead of water. However, close inspection of the metrical parameters shows that these differences lead to the cations of **2** and **3** not being superimposable. The Mn(1)−OH_2 bond

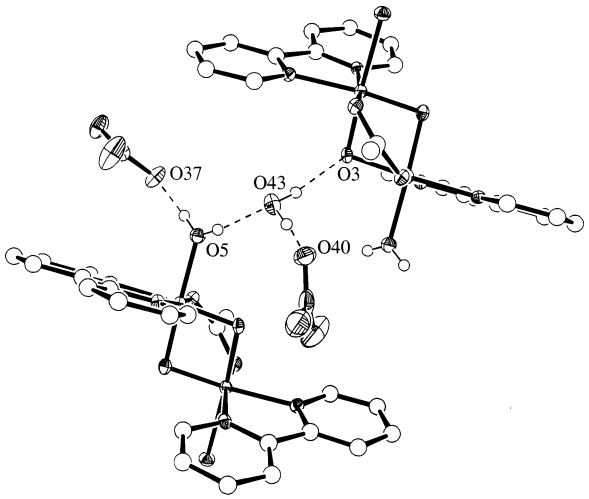

Figure 3. Two adjacent cations of **2** with O−H···O hydrogen-bonding interactions shown as dashed lines.

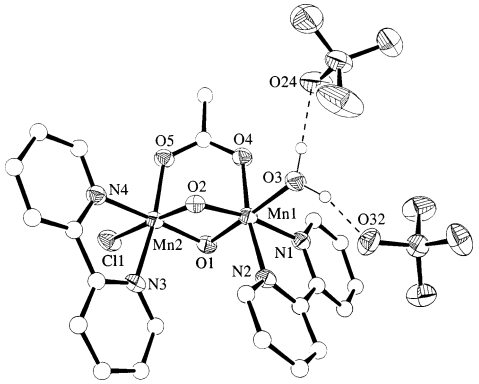

Figure 4. ORTEP representation of **3** at the 50% probability level showing O−H···O hydrogen bonds as dashed lines.

Table 4. Selected Interatomic Distances and Angles for **3**·MeCN[a]

Mn(1)−O(2)	1.783(2)	Mn(2)−O(1)	1.804(3)
Mn(1)−O(1)	1.791(2)	Mn(2)−O(2)	1.822(2)
Mn(1)−O(4)	1.925(2)	Mn(2)−O(5)	1.943(2)
Mn(1)−N(2)	1.993(3)	Mn(2)−N(3)	1.998(3)
Mn(1)−O(3)	2.002(3)	Mn(2)−N(4)	2.035(3)
Mn(1)−N(1)	2.047(3)	Mn(2)−Cl(1)	2.2512(11)
Mn(1)···Mn(2)	2.6524(8)		

O(2)−Mn(1)−O(1)	84.34(11)	O(1)−Mn(2)−O(2)	82.86(11)
O(2)−Mn(1)−O(4)	93.39(11)	O(1)−Mn(2)−O(5)	92.85(11)
O(1)−Mn(1)−O(4)	91.91(11)	O(2)−Mn(2)−O(5)	89.98(11)
O(2)−Mn(1)−N(2)	93.90(12)	O(1)−Mn(2)−N(3)	94.33(12)
O(1)−Mn(1)−N(2)	94.54(12)	O(2)−Mn(2)−N(3)	92.29(11)
O(4)−Mn(1)−N(2)	170.70(12)	O(5)−Mn(2)−N(3)	172.69(12)
O(2)−Mn(1)−O(3)	94.35(12)	O(1)−Mn(2)−N(4)	170.35(12)
O(1)−Mn(1)−O(3)	178.17(12)	O(2)−Mn(2)−N(4)	89.30(12)
O(4)−Mn(1)−O(3)	86.87(11)	O(5)−Mn(2)−N(4)	92.76(12)
N(2)−Mn(1)−O(3)	86.83(12)	N(3)−Mn(2)−N(4)	80.32(13)
O(2)−Mn(1)−N(1)	170.45(11)	O(1)−Mn(2)−Cl(1)	94.06(9)
O(1)−Mn(1)−N(1)	88.75(12)	O(2)−Mn(2)−Cl(1)	176.92(9)
O(4)−Mn(1)−N(1)	93.43(12)	O(5)−Mn(2)−Cl(1)	90.28(8)
N(2)−Mn(1)−N(1)	80.05(12)	N(3)−Mn(2)−Cl(1)	87.82(9)
O(3)−Mn(1)−N(1)	92.69(12)	N(4)−Mn(2)−Cl(1)	93.75(9)
Mn(1)−O(1)−Mn(2)	95.10(12)	Mn(1)−O(2)−Mn(2)	94.73(11)

[a] Distances are given in angstroms; angles are given in degrees.

length [Mn(1)−O(3) = 2.002(3) Å] of **3** is typical of literature values,[11l,13b,c] as mentioned above, but is significantly longer than the corresponding value in **2** [1.959(3) Å]. In addition, the Mn···Mn separation in **3**·MeCN [2.6524-

(24) Wieghardt, K.; Bossek, U.; Nuber, B.; Weiss, J.; Bonvoisin, J.; Corbella, M.; Vitols, S. E.; Girerd, J. J. *J. Am. Chem. Soc.* **1988**, *110*, 7398.

Table 5. Selected Structural and Magnetic Data for $[Mn^{IV}_2(\mu\text{-}O)_2(\mu\text{-}O_2CR)]^{3+}$ Complexes

		Mn···Mn (Å)	Mn−O−Mn (deg)	Mn−O (Å)	α (deg)	J (cm^{-1})	g	ref
1	$[Mn_2(\mu\text{-}O)_2(\mu\text{-}O_2CMe)Cl_2(bpy)_2]_2[MnCl_4]$	2.6715(11)	95.3(2)	1.807(4)	161.6	−45.0	2.00	TW[a]
2	$[Mn_2(\mu\text{-}O)_2(\mu\text{-}O_2CMe)Cl(H_2O)(bpy)_2]^{2+}$ [b]	2.6702(13)	94.8(2)	1.813(3)	161.8	−36.6	1.98	TW
3	$[Mn_2(\mu\text{-}O)_2(\mu\text{-}O_2CMe)Cl(H_2O)(bpy)_2]^{2+}$ [c]	2.6524(8)	94.9(1)	1.800(3)	162.5	−39.3	1.92	TW
7	$[Mn_2(\mu\text{-}O)_2(\mu\text{-}O_2CMe)(H_2O)_2(bpy)_2]^{3+}$ [c]	2.6401(5)	94.51(5)	1.797(1)	161.7	−43.7	1.98	13c
8	$[Mn_2(\mu\text{-}O)_2(\mu\text{-}O_2CMe)(H_2O)_2(bpy)_2]^{3+}$ [c]	2.642(3)	94.8(2)	1.794(4)	159.5	−67	2.00	13b
9	$[Mn_2(\mu\text{-}O)_2(\mu\text{-}O_2CMe)(bpea)_2]^{3+}$ [c,d]	2.580(1)	91.6(2)	1.799(4)	164.8	−124	2.29	13d
10	$[Mn_2(\mu\text{-}O)_2(\mu\text{-}O_2CMe)(bpta)_2]^{3+}$ [c,e]	2.6201(14)	93.2(2)	1.803(5)	161.7			13a
11	$[Mn_2(\mu\text{-}O)_2(\mu\text{-}O_2CMe)(tpen)_2]^{3+}$ [c,f]	2.591(1)	92.2(2)	1.798(3)	161.3			13e
12	$[Mn_2(\mu\text{-}O)_2(\mu\text{-}O_2CMe)(Me_4dtne)]^{3+}$ [c,g]	2.599(4)	92.6(4)	1.797(9)	159.3			12e
13	$[Mn_2(\mu\text{-}O)_2(\mu\text{-}HPO_4)(bpy)_2(H_2PO_4)_2]$	2.702(2)	96.5(4)	1.810(5)	164.5	−39.5	1.81	11o,p

[a] TW, this work. [a] Nitrate counterion. [c] Perchlorate counterion. [d] bpea = *N*,*N*-bis(2-pyridylmethyl)ethylamine. [e] bpta = *N*,*N*-bis (2-pyridylmethyl)-*tert*-butylamine. [f] tpen = *N*,*N*,*N*′,*N*′-tetrakis(2-pyridylmethyl)-1,2-ethanediamine. [g] dtne = 1,2-bis(1,4,7-triazacyclonon-1-yl)ethane.

(8) Å] is also similar to reported values[12e,13] but nevertheless is slightly shorter than that in **2** [2.6702(13) Å]. These differences can be assigned as due to the different hydrogen-bonding interactions in the two compounds. The situation in **2**·H_2O was described above. Examination of the unit cell of **3**·MeCN revealed hydrogen bonds between the bound water molecule and two perchlorate ions (Figure 4). However, there are no hydrogen bonds between the latter and a neighboring cation, and thus the cations are not bridged by hydrogen-bonded groups. The hydrogen bonds are O(3)···O(24) = 2.686(4) Å and O(3)···O(32) = 2.731(4) Å, with the O−H···O angles being 177(5)° and 156(5)°, respectively, values indicative of strong H-bonds. As for **2**·H_2O, the Mn_2O_2 unit of **3**·MeCN is not planar, the dihedral angle between the planes O(1)−Mn(1)−O(2) and O(1)−Mn-(2)−O(2) being 162.5(1)°, essentially identical with that in **2**.

Although there are quite a few dinuclear complexes with the $[Mn^{IV}_2O_2]^{4+}$ core, there is only a handful that have a bridging carboxylate group as well. These complexes, along with their pertinent structural parameters, are collected in Table 5. Within this family, complexes **1**−**3** are the first to possess both the $[Mn^{IV}_2(\mu\text{-}O)_2(\mu\text{-}O_2CR)]$ core and terminal Cl^- ligands. In addition, **1** and **2** possess an unusual asymmetry resulting from the different ligands (H_2O vs Cl^-) on the two Mn^{IV} ions. There are a few examples of asymmetric $[Mn_2(\mu\text{-}O)_2]^{3+/4+}$ compounds as a result of different binding modes adopted by the same bi-, tri-, or tetradentate ligands at the two ends of the molecule.[11j,k,n,12f] The only examples of Mn_2 complexes that are asymmetric owing to different ligands are the mixed valence (III/IV) complexes $[Mn_2O_2(\mu\text{-}O_2CMe)(O_2CMe)_2L]$ and $[Mn_2O_2(\mu\text{-}O_2CMe)L(bpy)(MeOH)](ClO_4)_2$ (where L = 1,4,7-trimethyl-1,4,7-triazacyclononane).[12d] Compounds **1** and **2** thus represent the first examples of asymmetric dimanganese(IV) complexes with the two Mn ions coordinated to different ligands.

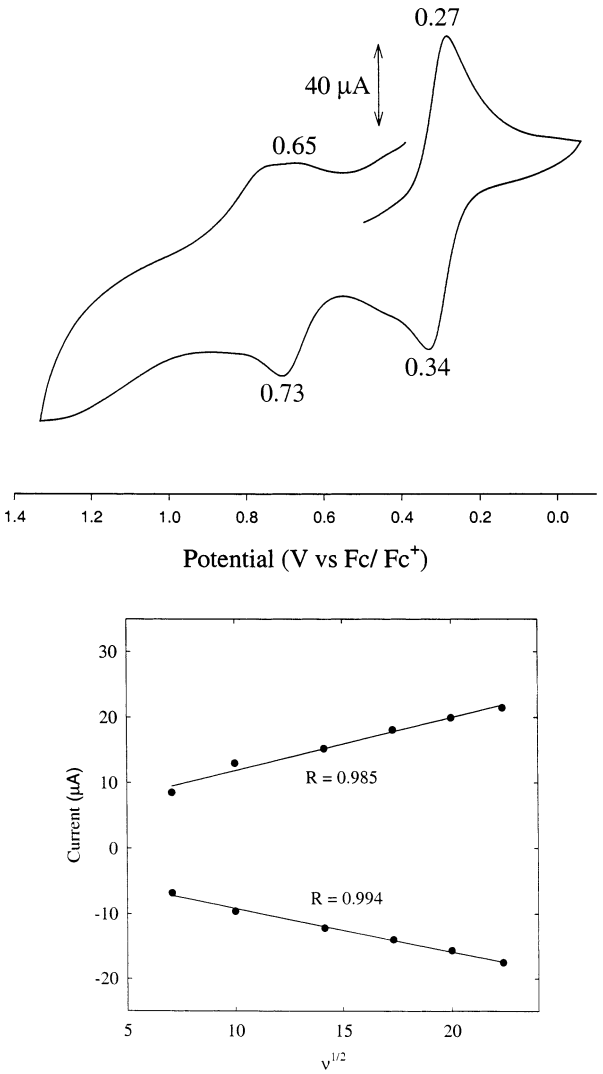

Figure 5. (Top) Cyclic voltammogram for complex **1** in MeCN; potentials are vs ferrocene under the same conditions. (Bottom) Plot of current vs $v^{1/2}$ for the reduction process.

Electrochemistry. The redox properties of complexes **1**−**3** were investigated by cyclic voltammetry (CV) in MeCN solution. The CV of **1** (Figure 5) displays an irreversible oxidation at $E_{1/2}$ = 0.69 V and a reversible reduction at $E_{1/2}$ = 0.30 V with peak separations at a scan rate of 100 mV/s of 80 and 70 mV, respectively. The ratio (i_f/i_r) of the forward and reverse currents for the two processes was 0.90 and 1.00, respectively. Plots of i_f and i_r vs $v^{1/2}$ for the reduction are linear in the scan rate (v) range of 10−500 mV/s (Figure 5), indicating a diffusion-controlled process. One additional irreversible reduction is seen at Ep_c = − 0.70 V. The irreversible oxidation process is assigned to the oxidation of the $[MnCl_4]^{2-}$ anion of **1**, and this was confirmed by the CV of $(BzEt_3N)_2[MnCl_4]$ recorded separately in MeCN. In particular, the latter also displays two poorly resolved peaks on the reverse (reductive) scan; this is consistent with a

chemical change to the $MnCl_4^{2-}$ anion after oxidation, as expected since Mn^{III} does not favor four-coordination, and multiple species appear to form as a result. In contrast, the reduction process is assigned to the cation of **1**:

$$\underset{(2Mn^{IV})}{[Mn_2O_2(O_2CMe)Cl_2(bpy)_2]^+} \rightleftarrows \underset{(Mn^{III},Mn^{IV})}{[Mn_2O_2(O_2CMe)Cl_2(bpy)_2]} \quad (3)$$

being reduced from the $2Mn^{IV}$ level to Mn^{III}, Mn^{IV}. Sweeps in the 0.0−0.5 V range emphasize the reversibility of this process.

In contrast to complex **1**, the CVs of **2** and **3** display only broad irreversible features. As expected, no oxidation couples were observed. However, only irreversible reductions were observed in cathodic scans, at approximately 0.33 and −0.55 V for **2**, and at 0.30 and −0.58 V for **3**, respectively. It thus appears that the bound solvent in **2** and **3** prevents the reversible reduction of **2** and **3**, possibly due to some subsequent chemistry following reduction and/or the strongly acidic nature of Mn^{IV}-bound H_2O, as confirmed in the corresponding symmetrical $[Mn_2O_2(O_2CMe)(H_2O)_2(bpy)_2]^{3+}$ species,[13b,c] which will be in equilibrium with the OH^--bound form. Similarly irreversible reduction couples in CV scans have been reported for $[Mn_2O_2(O_2CMe)(H_2O)_2(bpy)_2]^{3+}$,[13b] $[Mn_2O_2(terpy)_2(H_2O)_2]^{3+}$,[11l] and $[Mn_3O_4(bpy)_4(H_2O)_2]^{4+}$,[25] which also contain H_2O bound to Mn^{IV}.

Magnetic Susceptibility Studies. Measurements of the magnetic susceptibility of complexes **1**·1.5H_2O, **2**·H_2O, and **3**·H_2O were performed in the temperature range 2.00−300 K. The isotropic (Heisenberg) spin Hamiltonian for a Mn^{IV}_2 dimer is given by

$$\mathscr{H} = -2J\hat{S}_1\hat{S}_2 \quad (4)$$

where J is the exchange interaction parameter and $S_1 = S_2 = {}^3/_2$. This gives four total spin (S_T) states for the dimer of $S_T = 3$, 2, 1, and 0, whose energies $E(S_T)$ are the eigenvalues of eq 4 and are given by

$$E(S_T) = -JS_T(S_T + 1) \quad (5)$$

A theoretical χ_M vs T equation appropriate for a d^3-d^3 dimer has been previously derived from the use of eq 5 and the Van Vleck equation.[26] This expression was modified to include a fraction (p) of paramagnetic impurity (assumed to be mononuclear Mn^{II}), and temperature-independent paramagnetism (TIP). The latter was kept constant at 500×10^{-6} cm^3 mol^{-1} K for **1** and 300×10^{-6} cm^3 mol^{-1} K for **2** and **3**; the larger number for **1** reflects the larger number of Mn atoms in its formula. The resulting equation was used to fit the experimental χ_M vs T data for the three complexes.

The experimental data for **1** are plotted as $\chi_M T$ vs T in Figure 6. The $\chi_M T$ value decreases rapidly from 8.33 cm^3 mol^{-1} K at 300 K to 4.83 cm^3 mol^{-1} K at 40.0 K, and then slowly to 4.51 cm^3 mol^{-1} K at 10.0 K. Below this temperature, it again decreases rapidly to 3.60 cm^3 mol^{-1} K. These $\chi_M T$ values correspond to effective magnetic moment (μ_{eff}) values of 8.17, 6.22, 6.00, and 5.37 μ_B, respectively. These variable-temperature data for **1** are consistent with the result of the crystal structure and the presence of an antiferromagnetically coupled Mn^{IV}_2 cation and a separate, mononuclear Mn^{II} ($S = {}^5/_2$) anion. The decrease in $\chi_M T$ between 300 and 40.0 K reflects the depopulation of the $S > 0$ excited states of the cation, and the $\chi_M T \sim 4.5$ cm^3 mol^{-1} K at 10.0 K corresponds to the cation being in its $S = 0$ ground state and all paramagnetism being due to the Mn^{II} anion ($\chi_M T = 4.4$ cm^3 mol^{-1} K for $S = {}^5/_2$ and $g = 2$). The decrease at lower temperature is likely due to a combination of zero-field splitting of the $S = {}^5/_2$ spin manifold and weak antiferromagnetic exchange interactions between different Mn^{II} ions. The data for **1** were fit to the theoretical expression, modified to take into account a fixed Mn^{IV}_2:Mn^{II} ratio of 2:1. Data below 10 K were ignored. The obtained fit (solid line in Figure 6) gave $J = -45.0(4)$ cm^{-1}, $g = 2.00(2)$, and $p = 0.024$.

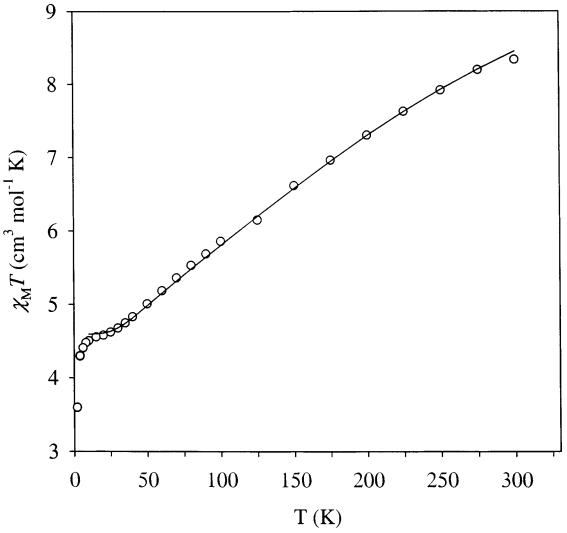

Figure 6. Plot of $\chi_M T$ vs T for **1**. The solid line is the fit of the data to the theoretical equation; see the text for the fit parameters.

The experimental data for **2** are plotted as $\chi_M T$ vs T in Figure 7. The $\chi_M T$ value decreases from 2.23 cm^3 mol^{-1} K at 300 K to 0.209 cm^3 mol^{-1} K at 40.0 K and then to 0.0028 cm^3 mol^{-1} K at 2.00 K. These correspond to μ_{eff} values of 4.22, 1.29, and 0.15 times μ_B, respectively. The decrease with decreasing temperature is again indicative of an antiferromagnetic exchange interaction between the two Mn^{IV} centers, and the fit of the data (solid line in Figure 7) gave $J = -36.6(4)$, $g = 1.97(1)$, and $p = 0.003(1)$.

The experimental data for **3** are plotted as $\chi_M T$ vs T in Figure 8. The $\chi_M T$ value decreases from 2.07 cm^3 mol^{-1} K at 300 K to 0.224 cm^3 mol^{-1} K at 40.0 K and then to 0.051 cm^3 mol^{-1} K at 2.00 K. These correspond to μ_{eff} values of 4.07, 1.34, and 0.64 μ_B, respectively. The fit of the data (solid line in Figure 8) gave $J = -39.3(4)$, $g = 1.92(1)$, and $p = 0.017(1)$.

The results of the fits confirm the presence of antiferromagnetic exchange interactions (negative J) between the two

(25) Sarneski, J. E.; Thorp, H. H.; Brudvig, G. W.; Crabtree, R. H.; Schulte, G. K. *J. Am. Chem. Soc.* **1990**, *112*, 7255.
(26) (a) O'Connor, C. J. *Prog. Inorg. Chem.* **1982**, *29*, 203−283. (b) *The Theory of Electric and Magnetic Susceptibilities*; Van Vleck, J. H., Ed.; Oxford University Press: London, 1932.

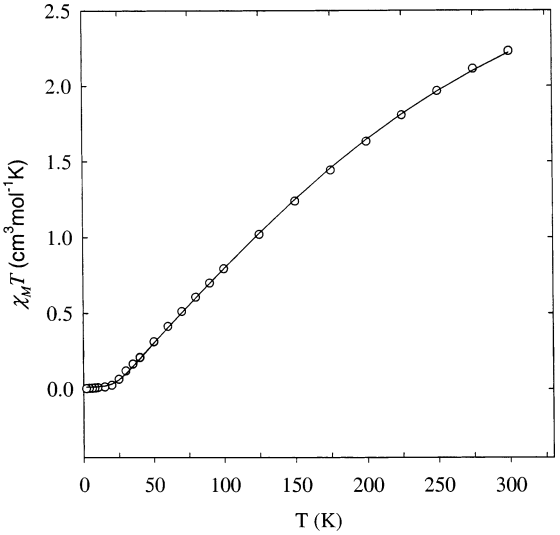

Figure 7. Plot of $\chi_M T$ vs T for **2**. The solid line is the fit of the data to the theoretical equation; see the text for the fit parameters.

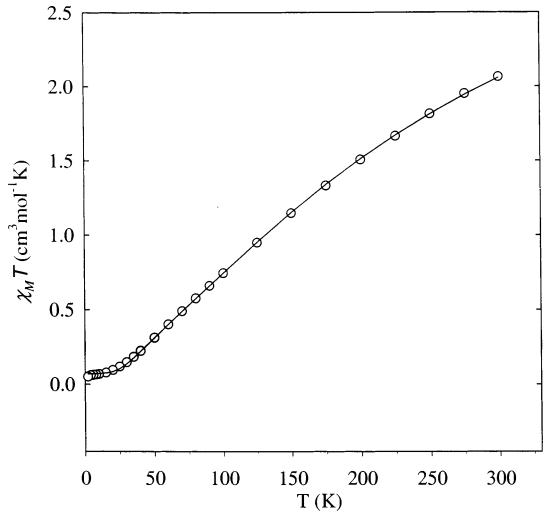

Figure 8. Plot of $\chi_M T$ vs T for **3**. The solid line is the fit of the data to the theoretical equation; see the text for the fit parameters.

Mn^{IV} ions in compounds **1**−**3** to give an $S_T = 0$ ground state. The obtained J values (−36.6 to −45.0 cm^{-1}) are similar to each other and to the values obtained for related compounds such as $[Mn^{IV}_2O_2(O_2CMe)(bpy)_2(H_2O)_2]^{3+}$ [13c] ($J = -43.7$ cm^{-1}) or $[Mn^{IV}_2O_2(HPO_4)(bpy)_2(H_2PO_4)_2]$ [11o,p] ($J = -39.5$ cm^{-1}) (Table 5). Recently, Pecoraro and co-workers reported a linear correlation between the Heisenberg exchange parameter (J) and the mean Mn−O−Mn angle of a number of $[Mn^{IV}_2(\mu\text{-}O)_2]$ complexes with iminophenolate ligands as well as non-Schiff-base ligands.[11a] The doubly bridged $[Mn^{IV}_2(\mu\text{-}O)_2]$ cores of all the compounds considered were planar. However, owing to the bridging acetate group, all compounds containing the triply bridged $[Mn^{IV}_2(\mu\text{-}O)_2(\mu\text{-}O_2CMe)]$ unit are not planar and thus are not expected to follow this linear correlation. Nevertheless, the Mn−O−Mn angles in these species are still expected to be at least one of the important factors determining the magnitude of J, and on this basis the obtained J values are consistent with the relatively acute Mn−O−Mn angles of ∼95°. This is emphasized by including the data points for **1**−**3** on the

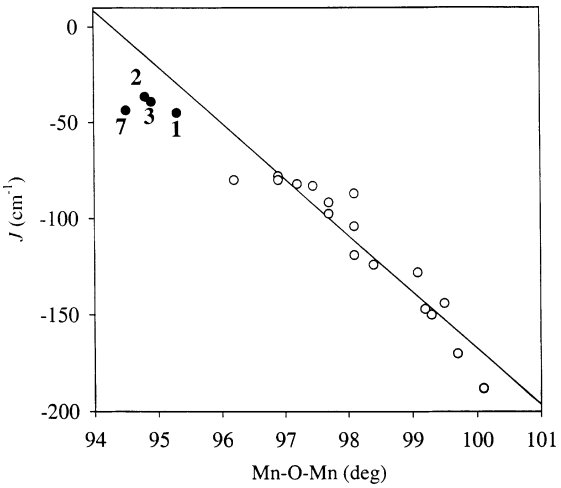

Figure 9. Plot of J (reciprocal centimeters) versus the Mn−O−Mn angle (degrees) for dinuclear complexes containing the $[Mn^{IV}_2O_2]$ core, adapted from ref 11a (○). (●) Data for compounds **1**−**3** and **7** of Table 5.

published plot of J vs Mn−O−Mn angles in doubly bridged $[Mn_2O_2]$ complexes (Figure 9). In addition, the reported J value for **7** (Table 5) is similar to those for **1**−**3**, whereas that for **8** is significantly stronger, and that for **9** seems incredibly large. Although the limited amount of data does not yet allow a good magnetostructural correlation to be established for compounds containing the triply bridged $[Mn^{IV}_2(\mu\text{-}O)_2(\mu\text{-}O_2CMe)]$ unit, the electronic structures and exchange parameters of a number of dinuclear complexes containing the $[Mn_2(\mu\text{-}O)_2(\mu\text{-}O_2CMe)]^{z+}$ ($z = 1, 2, 3$) core have been studied by DFT calculations, providing valuable insights into this class of complexes.[27] With more such compounds being synthesized, and structurally and magnetochemically characterized, it will hopefully become possible to elucidate all the factors that control the magnitude of the J value in this family of triply bridged complexes.

Conclusions

New examples of dinuclear manganese(IV) complexes with the $[Mn^{IV}_2(\mu\text{-}O)_2(\mu\text{-}O_2CMe)]^{3+}$ core have been prepared, and they represent the first examples of such complexes to also possess chloride ions as terminal ligands. Three of these complexes have been crystallographically characterized. Complex **1** is symmetric, but **2** and **3** are very rare examples of asymmetric dinuclear manganese complexes with the two Mn ions coordinated to different ligands and the first such examples for the $[Mn^{IV}_2(\mu\text{-}O)_2]$ core. These complexes could provide useful reference compounds in the future for Mn and Cl XAS and/or EXAFS studies designed to determine the site and mode of binding (terminal vs bridging) of cofactor Cl^- to the native WOC Mn_4 cluster.[28]

Magnetochemical studies of complexes **1**−**3** show that their exchange parameters (J) are all negative (antiferro-

(27) (a) Delfs, C. D.; Stranger, R. *Inorg. Chem.* **2001**, *40*, 3061. (b) Zhao, X. G.; Richardson, W. H.; Chen, J. L.; Li, J.; Noodleman, L.; Tsai, H. L.; Hendrickson, D. N. *Inorg. Chem.* **1997**, *36*, 1198. (c) Brunold, T. C.; Gamelin, D. R.; Stemmler, T. L.; Mandal, S. K.; Armstrong, W. H.; Pennerhahn, J. E.; Solomon, E. I. *J. Am. Chem. Soc.* **1998**, *120*, 8724.

(28) Rompel, A.; Andrews, J. C.; Cinco, R. M.; Wemple, M. W.; Christou, G.; Law, N. A.; Pecoraro, V. L.; Sauer, K.; Yachandra, V. K.; Klein, M. P. *J. Am. Chem. Soc.* **1997**, *119*, 4465.

magnetic), as expected, and are similar to each other and to those reported for related compounds in the literature. These values are consistent with the relatively acute Mn−O−Mn angles, but other factors are clearly also important in determining *J*. Nevertheless, the data for **1**−**3** roughly follow the linear *J* vs Mn−O−Mn angle correlation established for complexes with the doubly bridged, planar $[Mn^{IV}_2O_2]$ cores. This probably reflects the only small degree of deviation from planarity in the triply bridged $[Mn^{IV}_2O_2(O_2CMe)]$ cores of **1**−**3** (dihedral angle $\alpha = 159.3-164.8°$; see Table 5). Clearly, the synthesis and magnetostructural characterization of more compounds containing the $[Mn^{IV}_2(\mu\text{-}O)_2(\mu\text{-}O_2CMe)]$ core are needed before all the factors that control the *J* value can be established in this sub-branch of Mn^{IV}_2 complexes.

Acknowledgment. This work was supported by the University of Florida.

Supporting Information Available: X-ray crystallographic files in CIF format for complexes **1**·$2CH_2Cl_2$, **2**·H_2O, and **3**·MeCN (CIF). This material is available free of charge via the Internet at http://pubs.acs.org.

IC020570V